Farag *et al. Beni-Suef Univ J Basic Appl Sci* (2023) 12:57
https://doi.org/10.1186/s43088-023-00395-4

Beni-Suef University Journal of Basic and Applied Sciences

RESEARCH

Open Access

Thyroxine restores hippocampal neurogenesis and synaptogenesis in a male rat model of carbimazole-induced hypothyroidism: a histological study

Eman Abas Farag[1], Soheir Assaad Filobbos[1], Noha Mohammed Afifi[1], Shimaa Tarek Mahmoud[1] and Sarah Mohammed Alghandour[1*]

Abstract

Background Adult-onset hypothyroidism has a deleterious effect on hippocampal cognitive and memory functions. This study was performed to evaluate the possible therapeutic effect of thyroxine on hippocampus degeneration in an adult male rat model of carbimazole-induced hypothyroidism and the potentiality of spontaneous recovery. Thirty-two adult male albino rats were divided equally into four groups, as follows: I (control group), II (hypothyroidism group) received carbimazole (20 mg/kg) orally once daily for 4 weeks; III (recovery group) rats were managed as in group II, then left untreated for an additional 4 weeks to assess spontaneous recovery; and IV (thyroxine-treated group): hypothyroidism was induced as in group II, then rats received levothyroxine (20 µg/kg/day) orally for 4 weeks. Rats and their corresponding controls were sacrificed after 4 weeks in group II and after 8 weeks in groups III and IV. The levels of T3, T4, and TSH were measured. Hematoxylin and Eosin staining of thyroid and hippocampal sections was performed. Additionally, toluidine blue staining and immunohistochemical staining for PCNA, GFAP, and synaptophysin were applied to hippocampus sections. Both morphometric measurements and statistical analysis were performed.

Results Comparison of thyroxine-treated group with hypothyroidism and recovery groups revealed a significant reduction in TSH level and an increase in T3 and T4 levels, as well as improved histological architecture in both the thyroid and hippocampal sections. Hippocampal sections revealed a significant decrease in the mean area percent of GFAP, a significant increase in the mean number of PCNA-positive cells in the subgranular zone (SGZ); a niche for the adult neural stem cells (NSCs) in the hippocampus; and a significant increase in the mean area percent as well as the mean optical density of synaptophysin.

Conclusion Hippocampal degeneration is induced by hypothyroidism and can be restored by thyroxine replacement therapy, probably through neuronal cell preservation, synaptogenesis, and stimulation of neurogenesis in SGZ. On the other hand, spontaneous recovery from this degeneration was inadequate.

Keywords Hypothyroidism, Hippocampus, Levothyroxine, SGZ, Neurogenesis, PCNA, GFAP, Synaptophysin

*Correspondence:
Sarah Mohammed Alghandour
sarah_alghandour@cu.edu.eg
[1] Histology Department, Faculty of Medicine, Cairo University, Cairo, Egypt

1 Background

Thyroxine (T4) and triiodothyronine (T3), two thyroid hormones (THs), are crucial for the growth, development, and regulation of numerous metabolic processes [1]. Up to 5% of the global population suffers from adult

hypothyroidism, an endocrine condition. Of them, about 99% have primary hypothyroidism [2]. In the brain, THs play an essential role in neurogenesis, neuronal cell differentiation, neuroplasticity, and myelination [3]. A wide range of clinical neurological symptoms, including depression and memory and cognitive deficits, have been documented by patients with untreated hypothyroidism [4]. A high frequency of cognitive impairment was found in studies of adult hypothyroid individuals [5, 6].

Adult hippocampal neurogenesis in the dentate gyrus (DG) plays important roles in hippocampus functions, such as memory function and mood regulation. It is regulated by many environmental and cell-intrinsic factors [7]. Hippocampus is extremely sensitive to THs; therefore, the previously mentioned disorders were correlated with the damaging effect induced by hypothyroidism on hippocampal neurons and disruption of adult hippocampal neurogenesis [7, 8]. In hypothyroid disease, cell migration, proliferation, and synaptic transmission in the hippocampus could be affected with subsequent cognitive disturbance [9].

Therefore, thyroxine replacement treatment could be utilized to reverse and lessen the effect of hypothyroidism on hippocampus cells and the cognitive symptoms of hypothyroidism in addition to restoring serum levels of T3 and T4 to achieve clinical euthyroidism [10–12]. Carbimazole is an antithyroid drug used to treat hyperthyroidism. It is a methimazole derivative that the liver converts to methimazole. Treatment with carbimazole leads to decreasing levels of T3 and T4; therefore, carbimazole could be used to induce hypothyroidism [13]. Levothyroxine is a synthetic form of thyroxine hormone. It is also known as LT_4 and is regarded as the standard medication used to treat hypothyroid people [14].

Therefore, the aim of the current work was to develop an experimental model of hypothyroidism using carbimazole in an adult male albino rat. In such a model, the possible therapeutic effect of thyroxine on hippocampal degeneration as well as the possibility of spontaneous recovery were assessed. This was achieved by histological, immunohistochemical, and morphometrical studies.

2 Methods

2.1 Drugs

Carbimazole was purchased from CID Drug Company, Egypt, in the form of tablets; each tablet contains 5 mg carbimazole. Tablets were crushed, dissolved in distilled water, and administered orally via gastric tube once day for 4 weeks at a dose of 20 mg/kg [15].

Thyroxine (T4) (trade name Eltroxin): Was purchased as tablets from Glaxo Smith Kline Drug Company. Each tablet contains 50 µg of levothyroxine [dissolved in distilled water and given orally once daily for 4 weeks in a dose of 20 µg/kg/day] [16].

2.2 Animals

Thirty-two adult [nearly 90-day-old] male albino rats with an average body weight of 200 g were housed in the animal house & treated according to the guidelines of Cairo University Institutional Animal Care and Use Committee (CU-IACUC). The study Approval Number: CU-III-F-21-20. For acclimatisation, rats were put to a typical light/dark cycle and given free access to ordinary food and water for a week.

2.3 Experimental design

Rats were divided equally and randomly into four groups (I, II, III, and IV), 8 rats each.

Group I (Control group): rats received 0.5 ml of distilled water orally. They were subdivided into two subgroups:

Subgroup Ia (4 rats): sacrificed after 4 weeks [together with group II].
Subgroup Ib (4 rats): sacrificed after 8 weeks [together with groups III and IV].

Group II (Hypothyroid group) (Carbimazole treated): rats received carbimazole for 4 weeks, then were sacrificed.

Group III (Recovery group): rats were treated as in group II but sacrificed after a further 4 weeks (total of 8 weeks) to assess spontaneous recovery.

Group IV (Thyroxine-treated): hypothyroidism was induced by the same regimen as in group II, then rats received Eltroxin orally for a further 4 weeks before being sacrificed (total of 8 weeks).

2.4 Animal studies

2.4.1 Biochemical analysis

At the Biochemistry Department, tail vein blood samples were collected from all groups just before scarification for measuring T3, T4, and TSH by Enzyme Linked Immuno-Sorbent Assay (ELISA) (Biosource, TM, ELISA Kits, USA) [17].

2.4.2 Animal sacrifice and histological study

At The Laboratory Animal House Unit and Histology Department, rats were anaesthetized using an intraperitoneal injection of a combination of ketamine (80 mg/kg) & xylazine (10 mg/kg) [18]. The chest wall was opened, the descending aorta was tied off, and animals were transcardially perfused with 10% formol saline via the left ventricle in order to stabilize the brain in vivo to endure further processing. When

the venous return from the right atrium became clear perfusion was terminated [19]. The dissected brains of every rat were dehydrated in ascending alcohol concentrations for 24 h, embedded in paraffin, and fixed with 10% formol saline. Coronal sections were taken in series until the hippocampus was visible. From the left hippocampal region, 6 µm thick sections were cut. Additionally, a midline neck incision was made, the anterior neck muscles were separated, and the trachea was followed to the level of the thyroid gland in order to get a sample from the thyroid gland. After the thyroid gland was dissected, samples from the left lobe were preserved and processed into paraffin blocks. 6 µm thick thyroid sections were cut and stained by H&E [20].

The following stains were applied on hippocampal sections:

1. **Hematoxylin and Eosin stain (H&E)** [20].
2. **Toluidine blue stain** for demonstration of Nissl's granules [20].
3. **Immunohistochemical staining** for:

    a. **Proliferating Cell Nuclear Antigen (PCNA):** A mouse monoclonal antibody (Lab Vision Corporation Laboratories, CA 94539, USA, catalogue number MS-106-P). It appears as nuclear reactions in the proliferating cells [21].
    b. **Glial Fibrillary Acid Protein (GFAP):** A mouse monoclonal antibody (Lab Vision Corporation Laboratories, CA 94539, USA, catalogue number MS-1376-P). It appears as cytoplasmic reactions in astrocytes [22].
    c. **Synaptophysin:** It is a mouse monoclonal antibody appears as cytoplasmic reaction (Progen Biotechnic, Heidelberg, catalogue number 65012). Synaptophysin is a glycoprotein marker for synaptic activity at the pre-synaptic membranes [23].

Immunostaining using avidin–biotin technique requires pretreatment [20]. For antigen retrieval, sections were boiled for 10 min in 10 mM citrate buffer (Cat No. 005000) pH 6. Sections were left to cool for 20 min in room temperature. After that, sections were incubated with the primary antibodies for one hour. Immunostaining was finalized using Ultravision One Detection System (Cat No. TL-060-HLJ). Counterstaining was performed by Mayer's hematoxylin (Cat No. TA-060-MH). Citrate buffer, Ultravision One Detection System, and Mayer's hematoxylin were purchased from Labvision, ThermoFisher Scientific, USA.

2.4.3 Morphometric study

Leica Qwin 500 LTD image analyzer computer system (Cambridge, UK), at Histology Department, was used to measure:

- The thickness of pyramidal and granular layers in H&E- stained sections.
- The number of damaged neurons in the pyramidal and granular layers in H&E- stained sections.
- The number of PCNA positive immunoreactive cells in SGZ of DG
- The area percent of positive immunoreactivity for GFAP.
- The area percent and optical density of positive immunoreactivity for synaptophysin.

All measurements were done in ten non-overlapping, randomly selected high power fields (X400) for each animal in the control and experimental groups.

2.5 Statistical analysis

Biochemical results, as well as morphometric measurements, were tabulated and statistically analyzed. The statistical analysis included the arithmetic mean, standard deviation, and analysis of variance (ANOVA). The probability (P) value was directly provided by the computer using IBM SPSS (Statistical Package for Social Sciences) for Windows, Version 23.0. Armonk, NY: IBM Corp. P value < 0.05 was considered statistically significant.

3 Results

The biochemical, histological, and morphometric results of the control subgroups were comparable to each other and were collectively presented as group I (control group).

3.1 Biochemical results

3.1.1 Serum levels of T3 (ng/dl), T4 (µg/dl) and TSH (µg/dl)

Mean values of serum T3 and T4 showed a significant decrease in groups II and III compared with group I, a non-significant increase in group III compared with group II, a significant increase in group IV compared with groups II and III, and a non-significant difference between groups I and IV. Mean values of TSH recorded a significant increase in groups II and III compared with group I, a non-significant decrease in group III compared with group II, a significant decrease in group IV compared with groups II and III, and a non-significant difference between groups I and IV (Fig. 1).

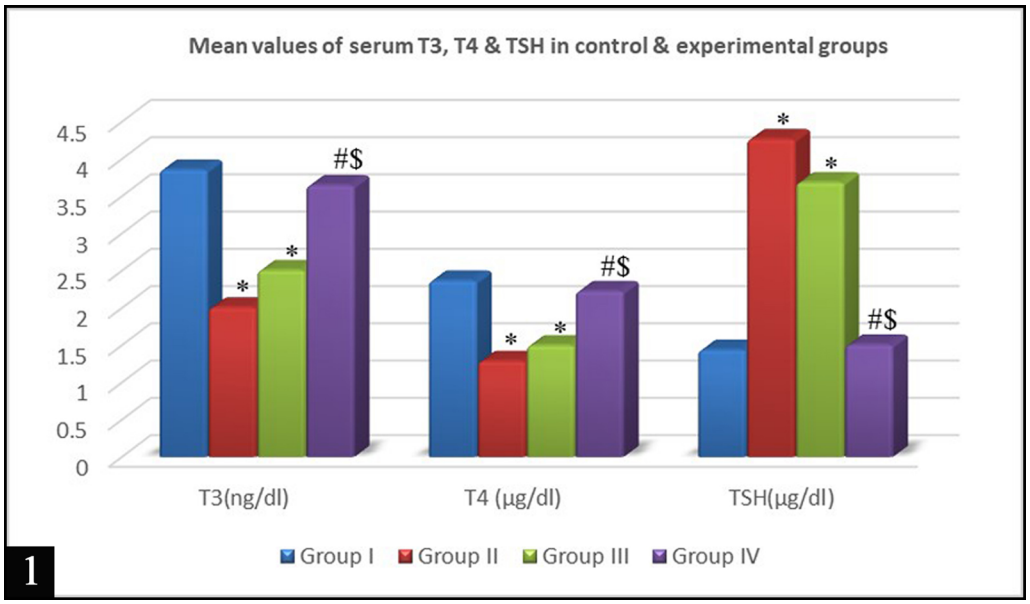

Fig. 1 Histogram showing the mean values of serum T3, T4 and TSH in all groups: significant compared to group I (*), group II (#), and group III ($) [significant difference at $P < 0.05$]

3.2 Histological results

3.2.1 Hematoxylin and eosin stained sections

3.2.1.1 Thyroid sections Histological examination of thyroid sections of the control group (group I) revealed the normal histological architecture of the thyroid gland. It was formed of variable-sized thyroid follicles. Each follicle was lined with a single layer of simple cubical epithelial cells, the follicular cells, exhibiting central rounded vesicular nuclei and basophilic cytoplasm. Follicles were filled with an acidophilic homogenous colloid with peripheral endocytic vacuoles. Follicles were surrounded by thin connective tissue and fenestrated blood capillaries. Parafollicular cells were noticed as paler and larger cells than the lining follicular cells and did not reach the lumina of the follicles or were seen in interfollicular tissue (Fig. 2a). Sections of both hypothyroidism group (group II) and recovery group (group III) showed enlarged follicles, partially or entirely devoid of colloid or exhibiting large endocytic vacuoles, most of them were lined with flat follicular cells with flattened nuclei, some cells were cubical and ballooned with vacuolated cytoplasm and rounded dark nuclei. Distorted follicles with some sequestered follicular cells from the basement membrane were also noted (Fig. 2b, c). Sections of thyroxine-treated group (group IV) revealed a nearly normal appearance of thyroid follicles comparable with control, apart from a few follicular cells with dark nuclei and vacuolated cytoplasm (Fig. 2d).

3.2.1.2 Hippocampal sections The control group revealed that hippocampus proper was formed of two main parts: Cornu Ammonis (CA) and dentate gyrus (DG). CA was subdivided into a superior part, which comprised CA1 and CA2, and an inferior part which comprised CA3 and its continuation, CA4, inside the concavity of the DG between its superior and inferior limbs forming the hilus. The dentate gyrus appeared as a dark C-shaped cap enclosing the free border of CA4. Areas inside the concavity of CA and outside the convexity of DG comprised the molecular layer (ML) (Fig. 3).

The present work illustrated the results of CA1, CA3, and DG examination, as the majority of histological alterations were clearly detected in these areas.

Examination of CA1 and CA3 regions of control group showed three main layers: (1) pleomorphic layer (OL), also known as stratum oriens, (2) pyramidal layer (PL), also referred to as stratum pyramidale, and (3) molecular layer (ML), which combines the strata known as stratum radiatum and lanculosum-moleculare. The main cellular layer was the PL, which was located between OL and ML. The dentate gyrus appears to be formed of superior and inferior limbs that merge at the end to form its characteristic C-shape. Each limb consisted of three layers: the outer dentate molecular layer (DML), the middle granular layer (GL) and the inner dentate pleomorphic layer (DOL). The same histological findings were observed on examination of the 3 layers of both limbs of the DG. Examination showed that PL neurons in both regions exhibited scanty basophilic cytoplasm and large, rounded vesicular nuclei with prominent nucleoli. PL neurons in CA1

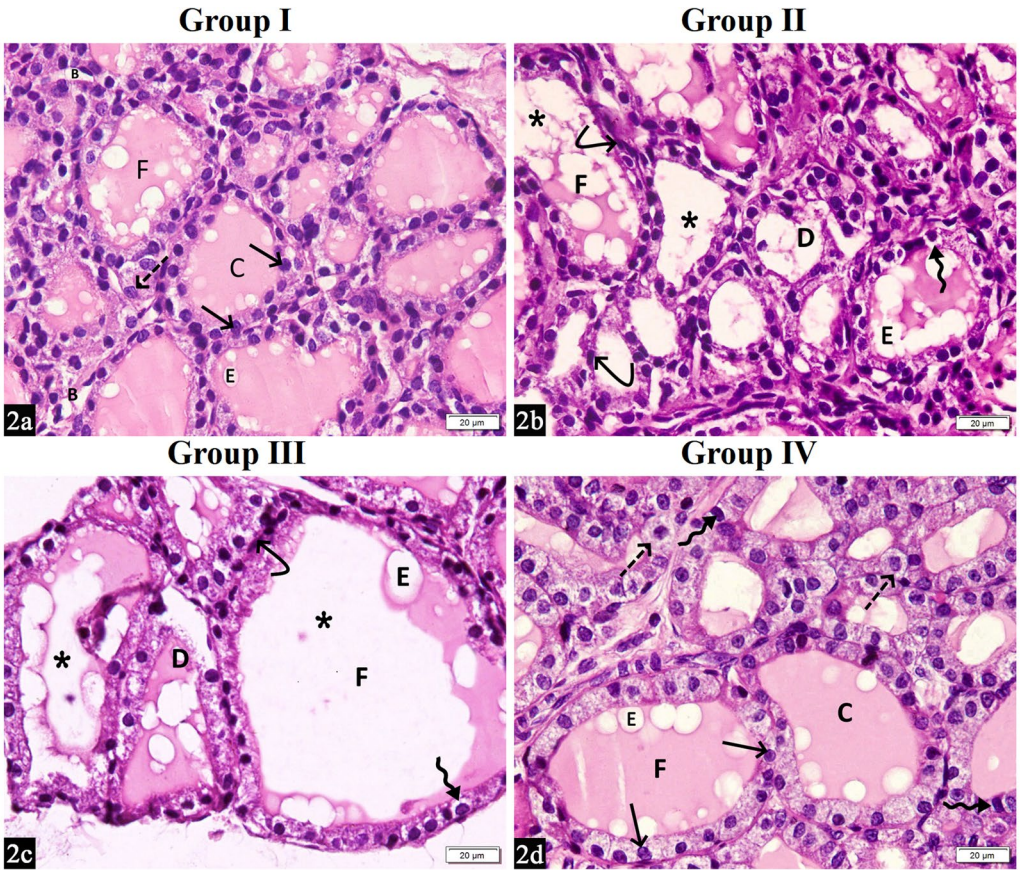

Fig. 2 Photomicrograph of sections in the thyroid gland of an albino rat from: **a** Control group demonstrating several thyroid follicles (F) of variable diameters, lined with simple cubical epithelial cells, follicular cells (arrows), exhibiting central rounded vesicular nuclei and basophilic cytoplasm. Follicles are filled with homogenous eosinophilic colloid (C) revealing peripheral endocytic vacuoles (E). Interfollicular tissue is formed of thin connective tissue with blood capillaries (B). Parafollicular cells (dashed arrow) are larger and paler than the lining follicular cells and do not reach the lumina of the follicles. **b**, **c** Both hypothyroidism (**b**) and recovery (**c**) groups are showing enlarged follicles (F) either partially or entirely devoid of colloid (asterisk) or exhibiting large endocytic vacuoles (E). Follicles are lined mainly with flat follicular cells with flattened nuclei (curved arrows). Some cells were cubical and ballooned with vacuolated cytoplasm and rounded dark nuclei (wavy arrow). Distorted follicles (D) with sequestration of some follicular cells from the basement membrane are also noted. **d** Thyroxin-treated group. Most of the thyroid follicles (F) are apparently normal, lined with simple cubical epithelial cells having central rounded vesicular nuclei (arrows) and parafollicular cells (dashed arrows). Follicles have an eosinophilic colloid (C) exhibiting several endocytic vacuoles (E). Few follicular cells with dark nuclei and vacuolated cytoplasm are noted (wavy arrows). [H&E, ×400]

were relatively smaller in size, and appeared closely packed, whereas in CA3 region, they were relatively larger and loosely packed. The GL constituted the principal layer of DG; it was formed of 4–6 rows of closely packed rounded granule cells exhibiting rounded vesicular nuclei and scanty basophilic cytoplasm. OL and ML of CA and DML and DOL of DG contained few neuroglial cells exhibiting small, rounded condensed nuclei, in addition to blood vessels in a pink neuropil background composed of neuronal and glial cell processes. It was noticed that small dark cells, variable in shape and size, were present in a narrow zone located between the hilus and the GL, known as the sub-granular zone (SGZ) (Fig. 4a–c**).**

Examination of hippocampal sections of groups II (hypothyroidism group) and III (recovery group) revealed marked histological changes in the pyramidal cells located in CA1 and CA3. These changes included an apparently reduced thickness of layers of pyramidal cells and GL of DG as compared to the control. It was slightly observed in group II sections and rather more obvious in group III sections. Most of the pyramidal cells and cells of GL exhibited an irregular, shrunken outline, deeply eosinophilic cytoplasm, darkly stained pyknotic nuclei, and were surrounded by pericellular halos. More apparent cellular damage and disorganization were observed in group III sections. Some areas of complete cell loss were observed. Clumping of neuronal processes was

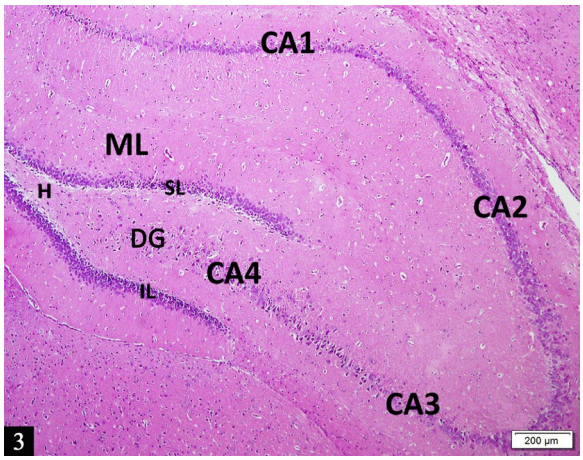

Fig. 3 A photomicrograph of H&E stained section in the left hippocampus from control group: CA1 and CA2 are in the superior region of Cornu Ammonis (CA), while CA3 and CA4 are in its inferior region. The dentate gyrus (DG) appears as a dark C-shaped cap surrounding CA4 by its superior and inferior limbs (SL and IL). CA4 is located inside the concavity of the DG, forming the hilus (H). Notice the presence of the molecular layer (ML) inside the concavity of CA and outside the convexity of DG. [H&E, X 40]

seen projecting into the ML and DML. Both ML and OL, as well as DML and DOL, showed an increase in glial cell content with small, rounded, deeply basophilic nuclei. Cells of SGZ in DG appeared as small dark cells, variable in shape and size, and were apparently reduced (Fig. 4d–i).

Histological examination of hippocampal sections of group IV (thyroxine-treated group) showed a return of histological features of hippocampal tissue toward normal morphology, which was comparable to the control sections. Restoration of most pyramidal and glial cells and markedly decreased degeneration were observed in CA1, CA3, and GL of DG regions, with obvious increase in the thickness of layers, as compared to sections of group II. Most pyramidal cells of CA1 and CA3 as well as cells GL of DG were characterized by having rounded vesicular nuclei with prominent nucleoli and scanty basophilic cytoplasm. Few cells were shrunken with an irregular outline, pyknotic, darkly stained nuclei, and deeply eosinophilic cytoplasm. Both ML and OL, as well as DML and DOL, contained few glial cells, blood capillaries, and neuronal and glial cell processes. SGZ appeared as a narrow layer of dark cells between the hilus and GL (Fig. 4j–l).

3.2.1.2.1 Toluidine blue stained sections

Histological examination of hippocampal sections of group I stained with toluidine blue showed normal structures of CA and DG. The pyramidal layer of both CA1 and CA3 showed pyramidal cells with large nuclei, and the granular layer of DG showed closely packed, rounded granular cells. All neurons had rounded vesicular nuclei, prominent nucleoli, and basophilic cytoplasm filled with Nissl's granules. Neuronal cell processes could be noticed (Fig. 5a–c).

Pyramidal cells in CA1 and CA3 and granular cells in DG showed great affection, as many of them in group II, and most of them in group III were irregular, dark with non-observable Nissl's granules, and clumping of neuronal processes. Some cells with rounded vesicular nuclei, prominent nucleoli and basophilic cytoplasm filled with Nissl's granules were seen. Neuronal cell processes and glial cells were noticed. In addition, some areas devoid of neuronal tissue were detected in group III sections (Fig. 5d–i).

Group IV sections showed that pyramidal cells of PL in CA1 and CA3 and granular cells of GL had rounded vesicular nuclei, prominent nucleoli, and basophilic cytoplasm filled with observable Nissl's granules. Some cells in CA and a few ones in DG were dark with

(See figure on next page.)

Fig. 4 A photomicrograph of H&E stained sections in the left hippocampus of different studied groups. **a**–**c** Control: **a** CA1 **b** CA3: PL (straight line); small, closely packed cells in (**a**) and loose, larger cells in (**b**). **c** SL of DG showing GL, closely packed rounded cells of 4–6 rows (straight line). Neurons with rounded vesicular nuclei & scanty basophilic cytoplasm (arrows). Note glial cells in ML, OL, DML, and DOL with small, rounded condensed nuclei (arrow heads), neuropil (black stars), and blood vessels (B). SGZ; narrow layer between hilus and GL; formed of small dark cells variable in size and shape (right angle arrows). **d**–**f** Group II & **g**–**i** group III: PL in CA1 (**d**, **g**), CA3 (**e**, **h**) and GL of DG (**f**, **i**): showing slight reduction in thickness (straight line) in group II and more apparent reduction in group III. Shrunken irregular pyramidal and granular cells with deeply eosinophilic cytoplasm and dark pyknotic nuclei (curved arrows), and pericellular haloes (dashed arrow). Notice areas devoid of neurons (square area), numerous glial cells (arrow heads) in ML, OL, DML, and DOL, blood vessels (B), clumping of neuronal processes (double arrows), and apparently reduced cells of SGZ (right angle arrow). **j**–**l** Group IV: PL in CA1 (**j**), CA3 (**k**) and GL of DG (**i**): exhibiting apparent increase in thickness (straight line) versus group II. Apparently normal neurons (arrows). Few shrunken neurons with eosinophilic cytoplasm and dark pyknotic nuclei (curved arrows). Note glial cells (arrow heads) in [ML, OL, DOL, and DML], blood capillaries (B), neuronal and glial cell processes (black star), and evident SGZ cells (right angle arrows). [H&E, X400]. **m** Histogram showing mean values of pyramidal layer thickness in CA1&CA3 and granular layer thickness in DG in all groups. **n** Mean number of damaged neurons in CA1&CA3 and granular layer in DG in all groups: significant versus group I (*), group II (#) & group III ($) [significant difference at $P < 0.05$]

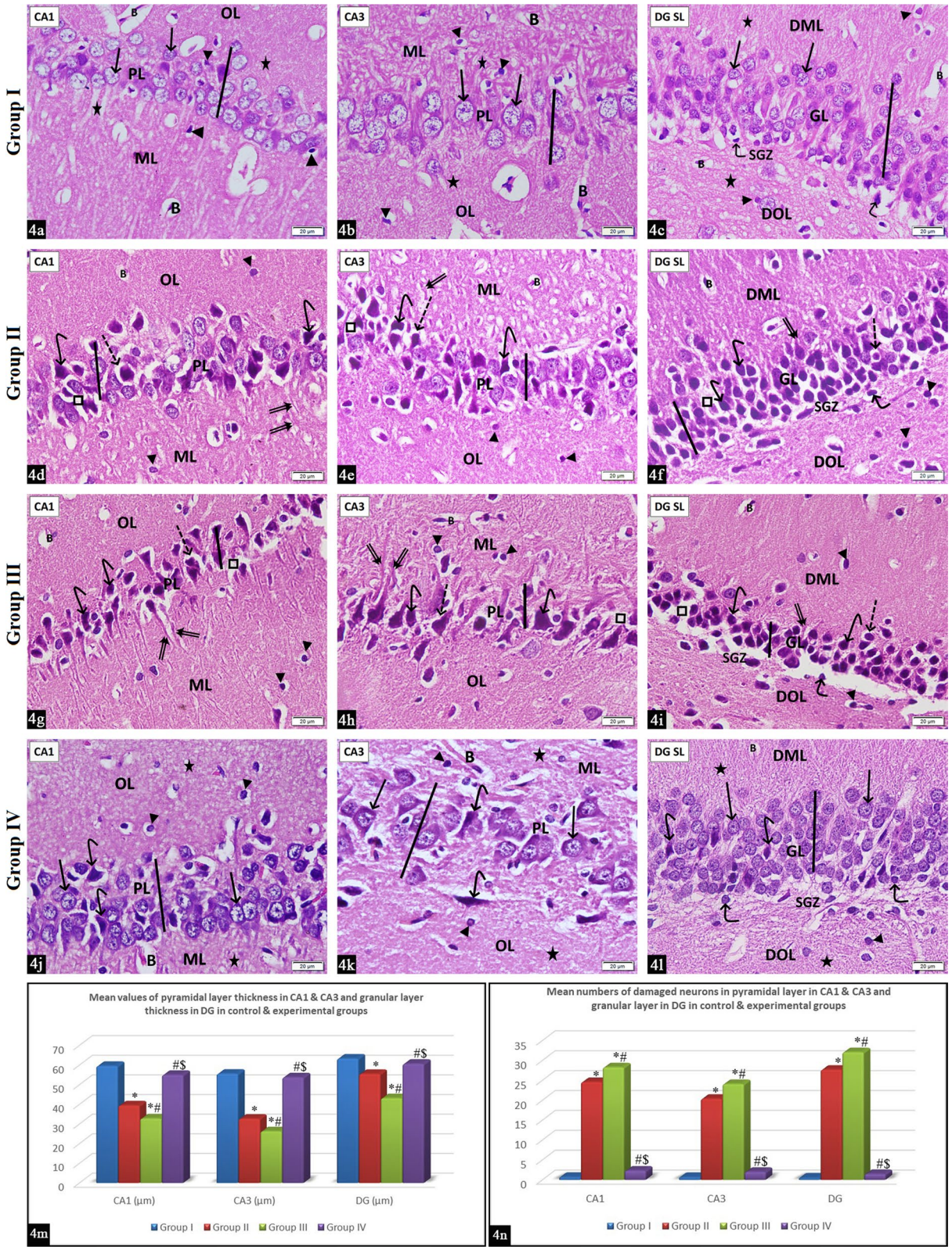

Fig. 4 (See legend on previous page.)

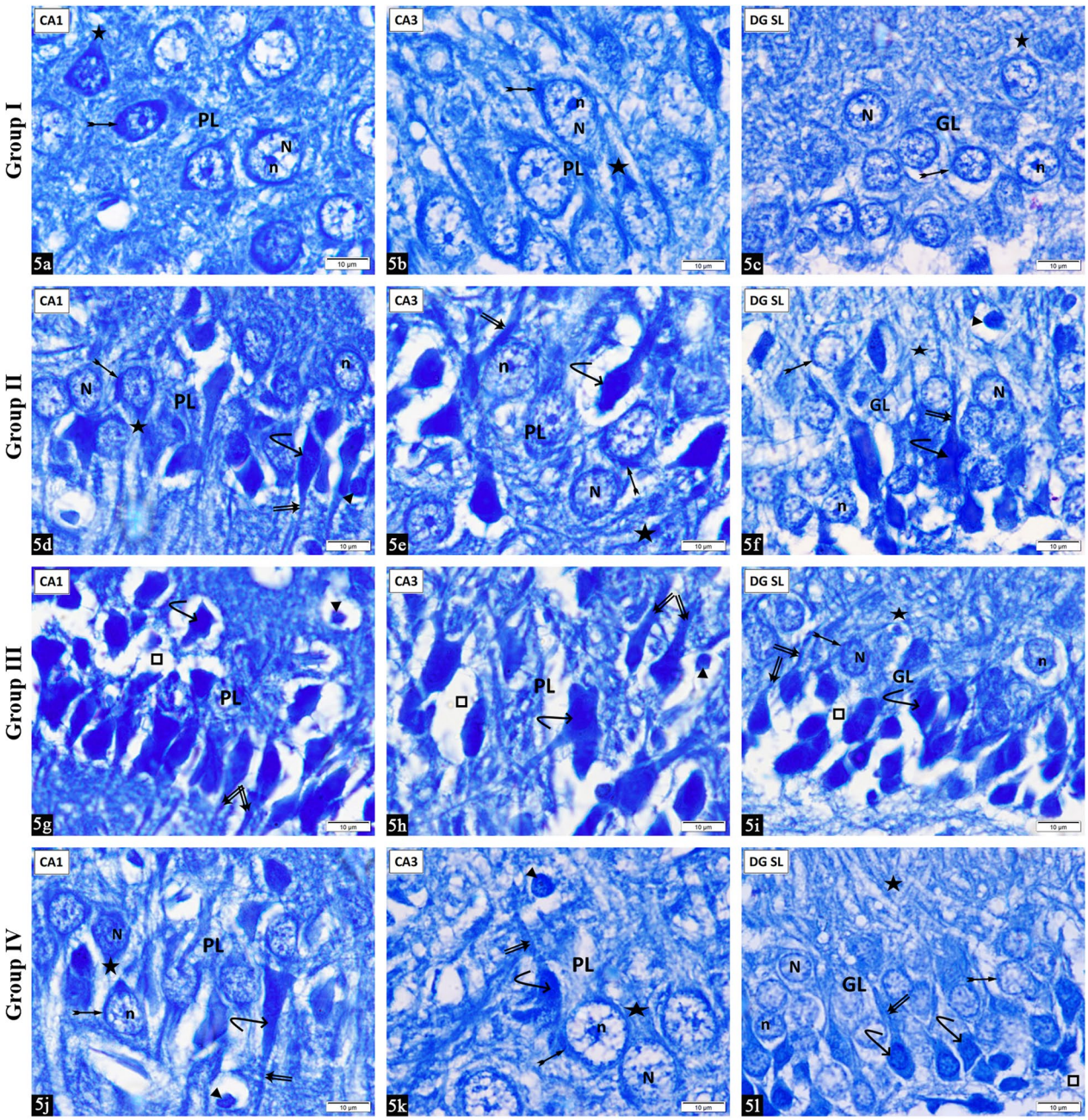

Fig. 5 A photomicrograph of toluidine blue-stained sections in the left hippocampus of different groups: **a**–**c** control: **a** CA1 and **b** CA3 regions showing cells of PL, and **c** SL of DG showing cells of GL. All neurons have large rounded vesicular nuclei (N) with prominent nucleoli (n). The cytoplasm is filled with Nissl's granules (bifid arrow). Neuronal cell processes are detected (black star). **d**–**f** Group II and **g**–**i** group III: **d**, **g** CA1 and **e**, **h** CA3 regions showing PL, and (**f**, **i**): DG showing GL. Many pyramidal cells in (**d**, **e**) and most of them in (**g**, **h**) as well as many granular cells appear irregular and dark with non-observable Nissl's granules (curved arrow). Clumping of neuronal cell processes (double arrows) is noticed. Some cells are normal, with rounded vesicular nuclei (N), and prominent nucleoli (n) and their cytoplasm is filled with Nissl's granules (bifid arrow). Neuronal cell processes (black star) and some glial cells are also detected (arrowhead). Some areas are devoid of neuronal tissue (square area) in (**g**–**i**). **j**–**l** Group IV: **j** CA1 and **k** CA3 regions showing PL, and **l** DG showing cells of GL. Many pyramidal cells and GL cells have rounded vesicular nuclei (N) with prominent nucleoli (n) and basophilic cytoplasm with observable Nissl's granules (bifid arrow). Neuronal cell processes (black star) are observed. Some cells in (**j**, **K**) and few ones in (**l**) are dark with non-observable Nissl's granules (curved arrow) and clumping of neuronal cell processes (double arrows). Glial cells are detected (arrowhead). Areas devoid of neuronal tissue are noticed (square area) in (**l**). [Toluidine blue, ×1000]

non-observable Nissl's granules and clumping of neuronal processes. Neuronal cell processes and glial cells were noticed. Areas devoid of neuronal tissues were noticed (Fig. 5j–l).

3.2.2 Immunohistochemical results

3.2.2.1 Immunostained hippocampal sections for PCNA: Examination of hippocampal sections of the control group (Fig. 6a, b), hypothyroid group (Fig. 6d, e), recovery group (Fig. 6g, h), and thyroxine treated group (Fig. 6j, k) revealed negative immunoreactivity in neurons of PL in CA1 and CA3. On the other hand, PCNA positive immunoreaction was detected in SGZ in DG in the nuclei of some cells in control group (Fig. 6c), a few cells in both hypothyroid (Fig. 6f) and recovery group (Fig. 6i) and numerous cells in thyroxine-treated group (Fig. 6l). Positive immunoreactions were also noticed in the nuclei of some glial cells in all groups.

3.2.2.2 Immunostained hippocampal sections for GFAP: Examination of hippocampal sections of group I showed positive immunoreactivity in cytoplasm and processes of astrocytes in ML, OL, and PL in CA1, CA3, and in DML, DOL, and GL of DG (Fig. 7a–c). Regarding groups II and III, they revealed widespread positive immunoreactivity (Fig. 7d–i). Meanwhile, an apparent decreased GFAP immunoreaction was demonstrated in group IV (Fig. 7j–l).

3.2.2.3 Immunostained hippocampal sections for synaptophysin: Examination of hippocampal sections of the control group showed widespread dense positive synaptophysin immunoreactivity in the cytoplasm of neurons in all three layers (PL, ML, and OL) in CA1 and CA3, as well as in DML, DOL and GL of DG (Fig. 8a–c). While in group II and III sections, scattered light positive immunoreactivity was noticed (Fig. 8d–i). Concerning sections of group IV, they revealed widespread, dense positive immunoreactivity (Fig. 8j–l).

3.3 Morphometric results

The mean values of pyramidal layer thickness in CA1, CA3 and the granular layer in DG (Fig. 4m) as well as the mean values of area percent (Fig. 8m) and optical density (Fig. 8n) of synaptophysin immunopositive reactions in the same analyzed areas showed significant decreases in groups II and III when compared with group I. The mean value of group III showed a significant decrease versus group II. A significant increase in group IV values was detected when compared with groups II and III while non-significant difference was detected when compared with group I.

The mean number of damaged neurons in the pyramidal layer in CA1 and CA3, and in granular layer in DG showed a significant increase in groups II and III when compared with group I. The mean value of group III was significantly higher compared to group II. A significant decrease in group IV values was detected when compared with groups II and III, and a non-significant difference was found when compared with group I (Fig. 4n).

The mean number of PCNA immunopositive nerve cells in SGZ of DG in group IV showed a significant increase when compared with groups I, II and III. Group III recorded a significant decrease in comparison with group II. Groups II and III showed significant decreases compared to group I (Fig. 6m).

The mean area percent values of GFAP immunopositive reactions in CA1, CA3, and DG showed a significant increase in groups II and III [with no significant difference in between] in comparison to group I. In contrast, the mean values of group IV recorded a significant decrease when compared to groups II and III and non-significant difference when compared with group I (Fig. 7m).

4 Discussion

Hypothyroidism, caused by an insufficient amount of circulating THs, is a common condition affecting nearly 10% of the overall population and becoming more prevalent with age [1, 11, 24]. Imbalance in THs is frequently associated with functional and structural brain alterations [25]. Due to the high expression of THs receptors in the hippocampus, it is particularly sensitive to the effects of THs [8]. Adult hippocampal neurogenesis has been implicated in cognitive processes such as learning and memory under normal physiological conditions. Consequently, dysregulation of adult hippocampal neurogenesis was associated with cognitive impairment [7]. To enhance the patient's quality of life, this impairment must be reversed. Therefore, the present study was designed to

(See figure on next page.)

Fig. 6 A photomicrograph of PCNA immunohistochemically stained left hippocampus sections. Positive PCNA nuclear immunoreactions in glial cells (arrow heads) and cells of the SGZ (dashed arrow): [**a**–**c** control group, **d**–**f** hypothyroidism group, **g**–**i** recovery group and **j**–**l** thyroxine-treated group]: Nerve cells of PL in CA1 (**a**, **d**, **g**, **j**) and CA3 (**b**, **e**, **h**, **k**) regions show negative immunoreactivity. **c**, **f**, **i**, **l** SL of DG shows positive immunoreactivity in the nuclei of some cells of SGZ in control (**c**), in few cells in groups II (**f**) and III (**i**), and in numerous cells in group IV (**l**). Immunopositive reactions are also seen in the nuclei of some glial cells. [Immunohistochemical stain for PCNA, ×400]. **m** Histogram showing the mean number of PCNA immunopositive nerve cells in SGZ of DG: significant compared to group I (*), group II (#), and group III ($), [significant difference at $P < 0.05$]

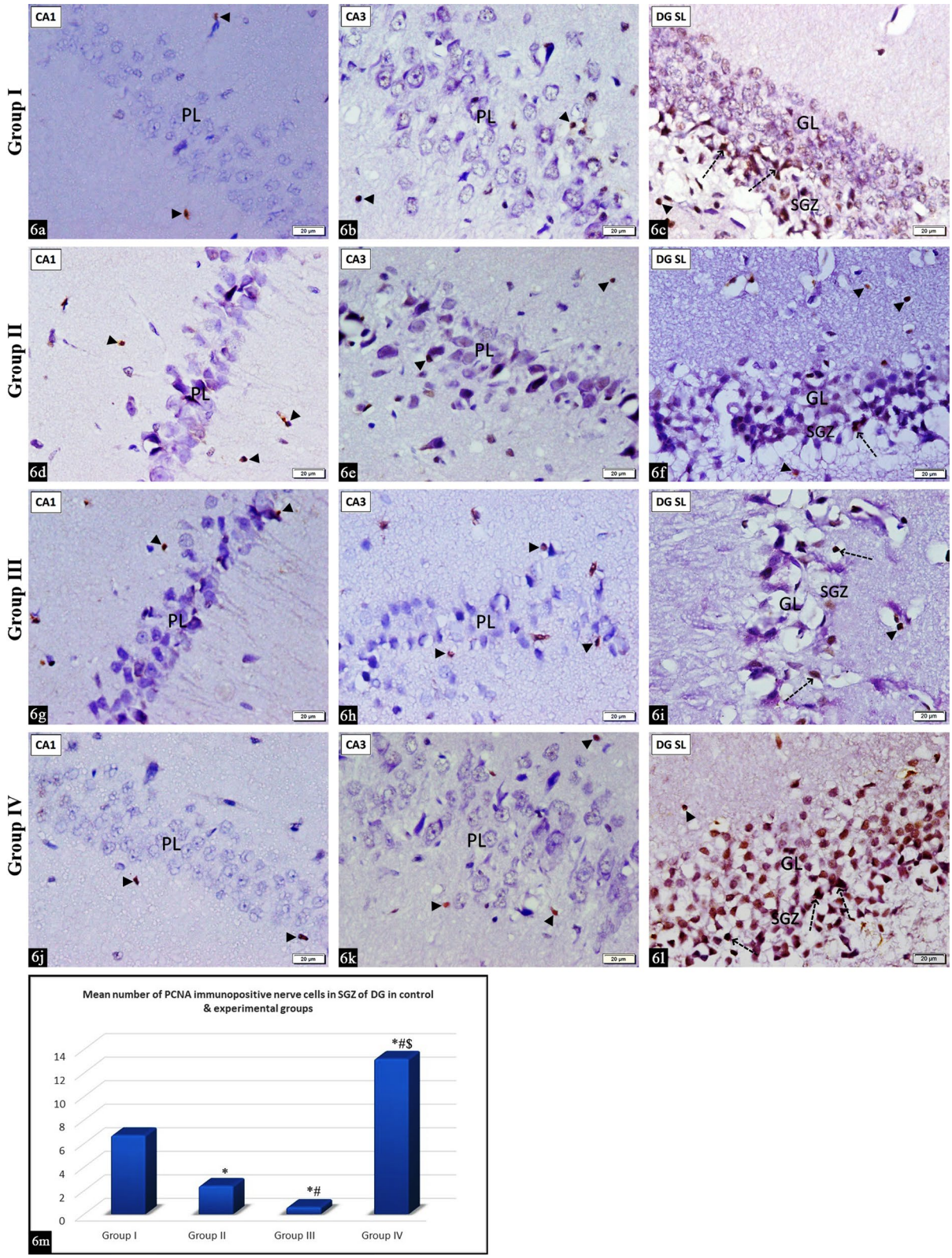

Fig. 6 (See legend on previous page.)

assess the potential effect of thyroxine on hippocampus degeneration induced by hypothyroidism.

In the present work, male rats were chosen to avoid hormonal fluctuations caused by the female estrous cycle [26]. The antithyroid medication carbimazole was employed to induce hypothyroidism since it had been used often in earlier research [27, 28] and because it is thought to be the best treatment for hyperthyroid individuals due to its low risk of side effects, particularly those affecting the gastrointestinal tract [29]. In the same consequence, levothyroxine (LT4) was chosen as replacement therapy as it has been established as the standard monotherapy for treatment of hypothyroidism [14]. The concern of the present work was the CA1, CA3, and DG regions, as they are the main components of the neural circuit in the hippocampus [trisynaptic pathway; DG to CA3 to CA1], which coordinates various hippocampal functions [30]. Also, these areas revealed most of the histological changes.

In the current study, the induction of hypothyroidism in group II was verified biochemically by serum level analysis of the thyroid hormone profile, which revealed a significant decrease in T3 and T4 with significant increase in TSH compared to the control group. This was in accordance with previous studies [28, 31]. Further confirmation came from the histological alteration noted in the examined H&E-stained sections of the same group, which revealed distension of most of the follicles with colloid; many follicular cells were flat with flat dark pyknotic nuclei. Some follicles were distorted with sequestered cells from the basement membrane. These changes were similarly reported, and they were attributed to increased oxidative free radicals and a decrease in the antioxidants [28, 32].

Additionally, this could provide an explanation for the neurodegenerative changes detected in H&E as well as the toluidine blue hippocampal sections of group II. Many nerve cells in PL and GL were shrunken with pyknotic nuclei and deeply eosinophilic cytoplasm, in addition to complete loss of cells in some areas, with subsequent reductions in the thickness of PL [in CA1 and CA3] and GL [in DG] as confirmed by morphometric measurements, which revealed a significant decrease versus the control group. In the hippocampus, THs deficiency caused oxidative stress and endoplasmic reticulum stress, which led to neuronal cell death and apoptosis [33]. In the same concern, neurodegeneration, indicated by the chromatolysis of Nissl's granules in PL and GL, is a reactive change that occurs in the cell body of damaged neurons. These results were similarly described and explained by damage of the endoplasmic reticulum as a result of a deficiency of THs, which increased expression of apoptotic genes and enhanced DNA fragmentation [33–35].

More reinforcement came from the significant increase in the mean number of damaged neurons in the PL of CA1 and CA3 and the GL of DG in group II compared with the control group. These results are consistent with earlier research that found fewer pyramidal neurons in all areas of the hypothyroid hippocampus that were examined [36–38].

Thyroid hormones affect the behavior of neural stem cells (NSCs) in the adult brain [39]. Therefore, an important aim of the present study was to detect the effect of hypothyroidism on proliferating cells in the SGZ of DG. Adult neurogenesis in the SGZ is an extremely structured process that starts with NSCs, which produce proliferative progenitor cells and differentiate into post-mitotic immature granule cells and finally into mature granule cells. Normally, these cells preserve the capability to produce new neurons all through adult life [40, 41], which clarified the PCNA-positive immune reactivity seen in the control group of the present work. Cells of SGZ in group II were apparently reduced and demonstrated a significant decrease in the mean number of PCNA-positive neurons compared to the control group, confirming the capability of adult-onset hypothyroidism to decrease neurogenesis in the dentate gyrus. Hypothyroidism increased proinflammatory levels of cytokines [TNF-α, IL-6, IL-1β] and inflammatory markers in the hippocampus [C-reactive protein and COX-2], which suppress neurogenesis [31, 42].

The inflammation induced by hypothyroidism was paralleled in the same group by widespread positive GFAP immunoreactivity of astrocytes in all layers of CA1, CA3, and DG, which recorded a significant increase in the mean area percent compared with the control group. Such an increase was also noticed as numerous glial cells in H&E and positive PCNA immunoreactivity in PCNA immunostained sections. Although astrocytic gliosis is a sign of pathological changes in the nervous system, evidence suggests that gliosis is a protective reaction of the

(See figure on next page.)

Fig. 7 A photomicrograph of GFAP immunohistochemically stained sections in the left hippocampus. Positive GFAP immunoreactivity in cytoplasm and processes of astrocytes (dotted arrows) of PL, ML, and OL in CA1&CA3 and in DOL, DML and GL of DG: [**a**–**c** control group, **d**–**f** hypothyroidism group, **g**–**i** recovery group and **j**–**l** thyroxine-treated group)]: **a**, **j** CA1, **b**, **k** CA3 and **c**, **l** SL of DG showing positive immunoreactivity. **d**, **g** CA1, **e**, **h** CA3 and **f**, **i** SL of DG showing widespread positive immunoreactivity. [Immunohistochemical stain for GFAP, ×400]. **m** Histogram showing the mean area percent values of GFAP immunopositive reaction in CA1, CA3 and DG: significant compared to group I (*), group II (#), and group III ($), (significant difference at $P < 0.05$)

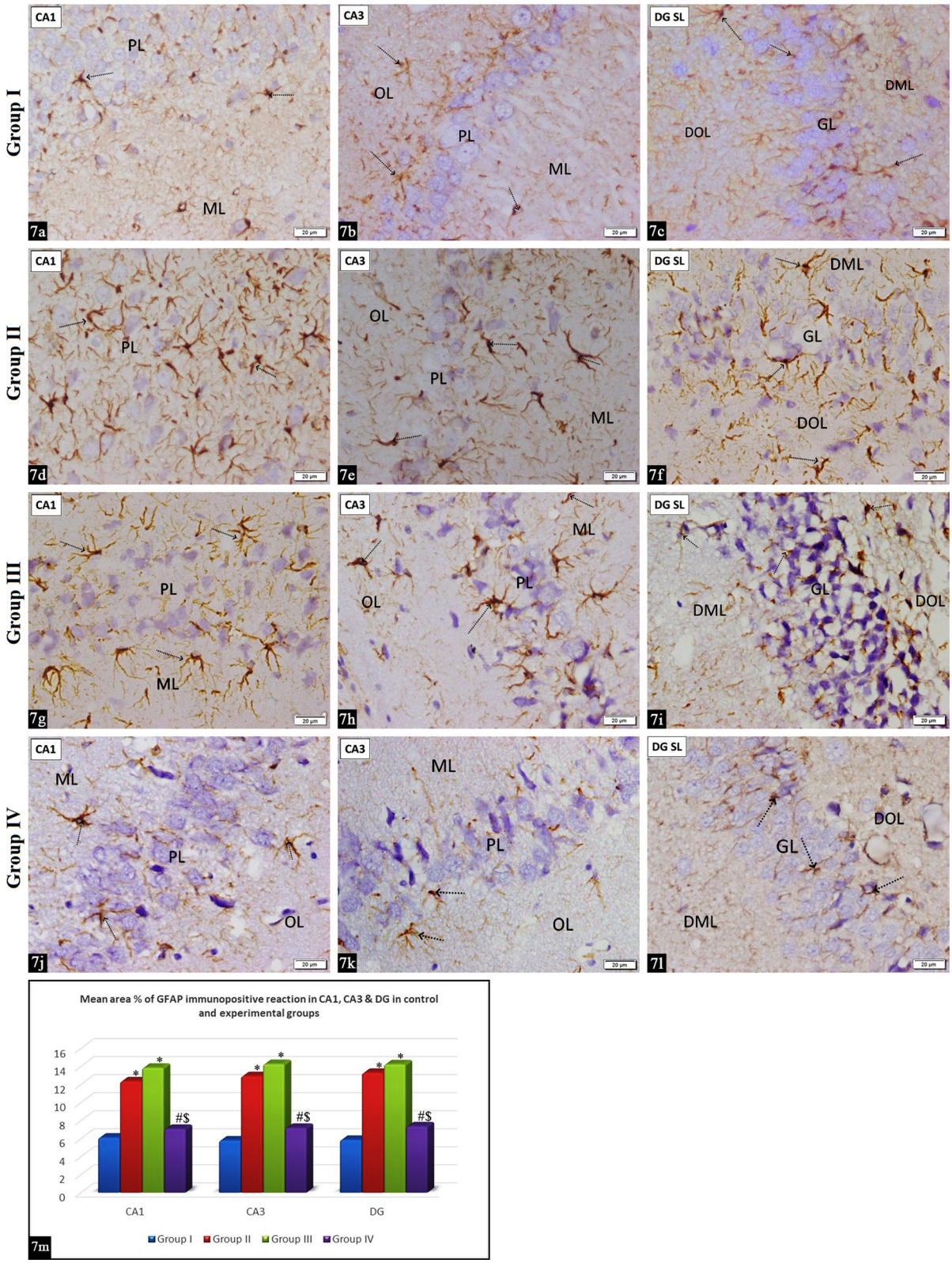

Fig. 7 (See legend on previous page.)

CNS against different types of damage, so the astrocytes increase in cases of brain inflammation, struggling to localize it [43, 44]. Another explanation for this increase could be the attempt of astrocytes to increase THs levels in the brain. Astrocytes play a central role in THs metabolism since they are the principal transporters of thyroxine from the blood, responsible for its conversion to 3,5,3′-triiodothyronine, and hence supplying the neural tissues with the biologically active form of the hormone [45–47].

Synaptophysin is an integral protein of small pre-synaptic vesicles that is involved in the release of neurotransmitter vesicles [48], so it was selected to assess synaptic formation. Synaptophysin immunostained sections of group II demonstrated mild positive immunoreactivity in the cytoplasm of neurons in all layers of CA1, CA3, and DG. A significant decrease in both mean area percent and optical density was demonstrated compared with the control group. This downregulation reflected deficits in synaptic formation due to hypothyroidism [49] and explained the commonly reported changes in the plasticity of the cell signaling pathway in the hippocampus and the subsequent deficits in memory [50].

Also, the reactive gliosis noticed in this group could be involved to a certain extent in such impairment. Normally, astrocytes aid synaptogenesis by forming and releasing crucial factors such as cholesterol and glypicans [51]. On the other hand, reactive astrocytes were reported to have aberrant calcium dynamics, which promote the release of detrimental factors that change neuron-glia communication and impair synaptic transmission and plasticity [52].

The current study recorded a trial of functional improvement in the thyroid gland following withdrawal of carbimazole in the recovery group (group III). This was supported by the recorded increase, although still non-significant, in the mean values of T3 and T4, and the decrease in TSH in group III versus group II and the significance differences when compared to the control, all of which pointed to persistent hypothyroidism. These findings were consistent with previous results [11]. Additionally, examination of thyroid sections demonstrated a nearly similar picture to group II. The stress exerted on cells by carbimazole just started to decline following its withdrawal. A longer period might be needed for a better recovery assessment.

Concerning H&E and toluidine blue-examined hippocampus sections in group III, they demonstrated almost similar findings to the hypothyroid group, with more progressive histopathological changes in the PL of CA1 and CA3 and in the GL of DG. Compared with group II, they verified a significant increase in the mean number of damaged neurons. It also recorded a significant decrease in the thickness of PL and GL, the mean number of PCNA-positive cells in SGZ, as well as the mean area percentage and optical density of synaptophysin. In the brain, just a trivial deviation from the normal range of brain T3 triggered widespread effects on nervous tissue [53]. Based on what's been mentioned previously, the present work suggests that the slight improvement recorded in serum T3 level in group III failed to achieve the required improvement in T3 brain level. This suggestion might provide an explanation for the persistent hippocampal alteration detected in the recovery group.

By contrast, the thyroid hormone profile in the thyroxine-treated group (group IV) established a significant increase in the levels of T3 and T4 and a decrease in TSH compared with groups II and III, and a non-significant difference when compared to the control group indicated the restoration of the euthyroid state. This agreed with previous results [28, 54]. The improvement in the hormonal profile in the current study was paralleled by the nearly normal appearance of the H&E stained thyroid gland. The majority of the follicles were lined with cubical cells with rounded vesicular nuclei and basophilic cytoplasm and filled with acidophilic colloid.

The improvement of thyroid gland structure and function in group IV was mirrored in the hippocampus, which showed reasonable restoration of normal histological features. Many pyramidal cells in CA1 and CA3 and granule cells in GL appeared normal with vesicular nuclei and basophilic cytoplasm filled with Nissl's granules, whereas few cells were shrunken with pyknotic nuclei and eosinophilic cytoplasm. Such amelioration was confirmed by morphometric studies that revealed a significant increase in the mean thickness of PL and GL compared with groups II and III, and a non-significant difference when compared with the control group. Also, the mean number of damaged neurons in PL and GL demonstrated a

(See figure on next page.)

Fig. 8 A photomicrograph of synaptophysin immunohistochemically stained sections in the left hippocampus. Positive synaptophysin immunoreactivity in the cytoplasm of neurons (wavy arrows) of PL, ML, and OL in CA1 & CA3 and in DOL, DML, and GL of DG: [**a**–**c** control group, **d**–**f** hypothyroidism group, **g**–**i** recovery group and **j**–**l** thyroxine-treated group]: **a**, **j** CA1, **b**, **k** CA3 and **c**, **l** SL of DG showing widespread dense positive immunoreactivity. **d**, **g** CA1, **e**, **h** CA3 and **f**, **i** SL of DG showing scattered light positive immunoreaction. [Immunohistochemical stain for synaptophysin, ×400]. **m** Histogram showing values of mean area percent of synaptophysin immunopositive reaction in CA1, CA3 & DG. And **n** Mean values of optical density of synaptophysin immunopositive reaction in the same areas: significant compared to group I (*), group II (#), and group III ($), (significant difference at $P < 0.05$)

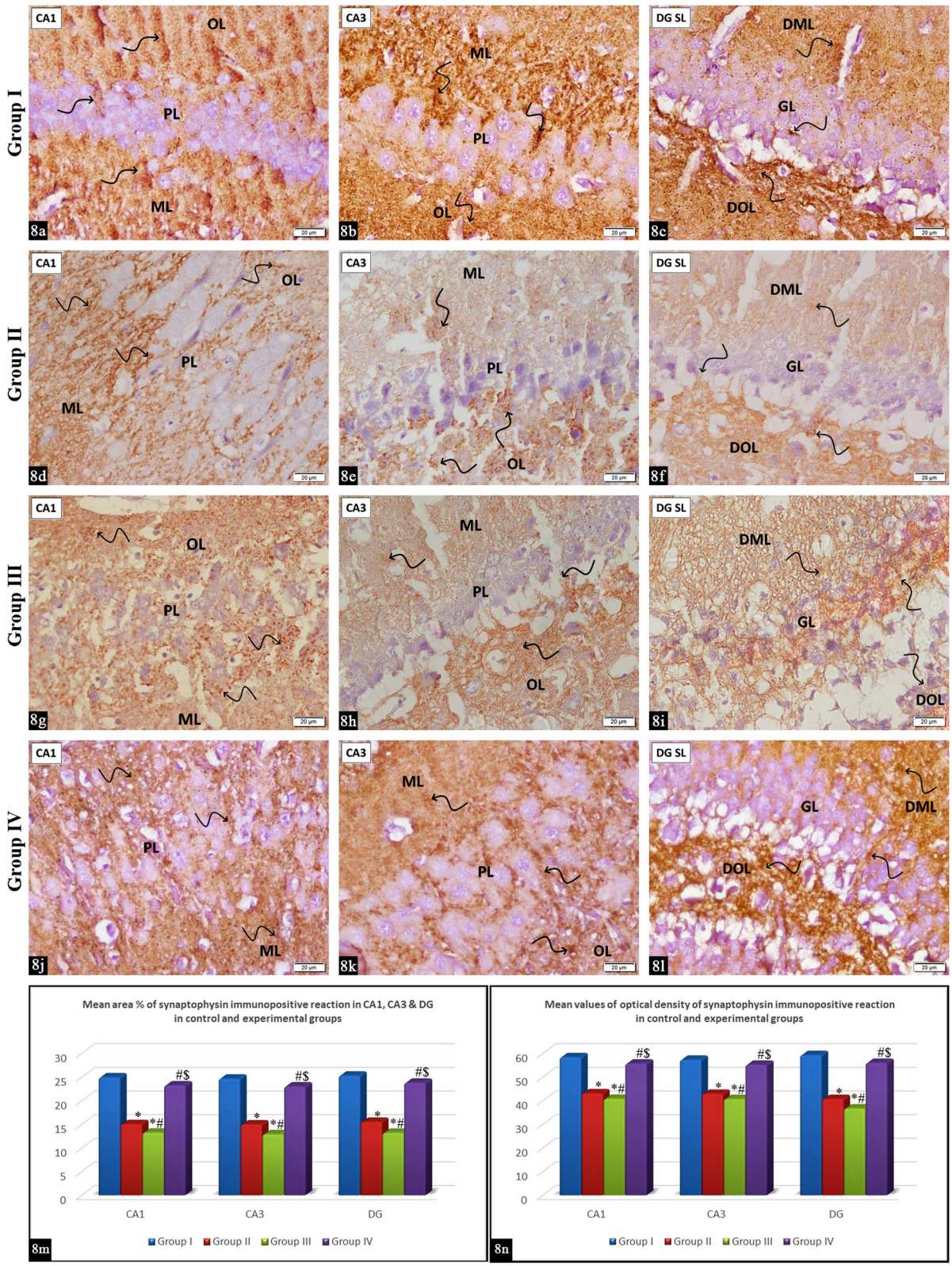

Fig. 8 (See legend on previous page.)

significant decrease when compared with groups II and III, and a non-significant difference when compared with the control group. Such improvement agrees with previous results [55, 56] and was attributed to the thyroxine treatment, which inhibits cell apoptosis and promotes neuronal cell survival and plasticity by improving oxidative stress in the hippocampus of hypothyroid rats [57] and by restoring the levels of brain-derived neurotrophic factor (BDNF), which regulates apoptosis in nervous tissue [58, 59].

In the current work, PCNA-immunostained sections of group IV revealed positive immunoreactivity in many cells in SGZ. This was further confirmed by morphometric results, which demonstrated a significant increase in the mean number of PCNA-positive cells in SGZ compared to groups II and III. Restoration of hippocampal neurogenesis in this group could be linked to the restored levels of T3 and T4, which, in turn, influence the proliferation of neural progenitor cells, the migration of neural cells, and their growth and survival [60]. Knowing that these newly formed neurons eventually become granular cells of DG [61], this may well explain the apparently normal GL of DG and the significant increase in its thickness. Likewise, replacement treatment with THs resulted in a statistically significant increase in the total number of both BrdU and Ki67 immunopositive proliferating cells in the SGZ of hypothyroid rats treated with thyroxine [62].

The increase in the mean number of PCNA-positive cells in SGZ in group IV compared to control was explained by the ability of these progenitor cells in the hippocampal neurogenic niche to increase their proliferation and the survival of newly generated neurons [more than in a resting or non-stressful state] as a response to variable stresses [63] to compensate for cells lost by inflammation and apoptosis induced by hypothyroidism.

GFAP immunostained sections from group IV revealed a significant decrease in the mean area percent of GFAP compared to groups II and III and a non-significant difference compared to the control group. This reduction could be explained by the regression of the neuroinflammation induced by hypothyroidism, with a subsequent decrease in astrocytes and GFAP. This assumption was confirmed in previous studies [11, 64], but other experiments have argued against it [56].

The present work assumed that treatment with levothyroxine could restore and protect synapses and dendritic processes in the hippocampus. Such an assumption was confirmed by densely positive synaptophysin immunoreactivity in the cytoplasm of neurons in CA1, CA3, and DG and by a significant increase in its mean area percent and optical density compared with groups II and III, and a non-significant difference when compared with the control. These results enforced the restoration of synaptic plasticity as the levels of synaptophysin expression paralleled the numbers of synapses and the density and quantity of nerve terminals [23, 65]. This could also be aided by the newly formed granular cells from NSCs in the SGZ of DG, which create new connections to support CNS plasticity [61]. Such restoration explained the reported improvement of cognitive impairment with hypothyroidism [24].

5 Conclusions

The present work concluded that hypothyroidism had a neurodegenerative effect on the hippocampus and decreased NSCs proliferation in SGZ. In addition, treatment with levothyroxine restored the normal range of thyroid hormones and restored hippocampal recovery, neurogenesis, and synaptogenesis, a finding with important implications for a broad spectrum of neurological disorders that entail compromised neurogenesis.

The present study's limitation was the need for additional functional and neurophysiological testing, despite the fact that the hippocampus's restored histological neurogenesis was shown at the histological level. Further investigation is advised as a result.

Abbreviations

THs	Thyroid hormones
T4	Thyroxine
T3	Triiodothyronine
LT4	Levothyroxine
SGZ	Subgranular zone
NSCs	Neural stem cells
DG	Dentate gyrus
ELISA	Enzyme linked immuno-sorbent assay
PCNA	Proliferating cell nuclear antigen
GFAP	Glial fibrillary acid protein
ANOVA	Analysis of variance
P	Probability
SPSS	Statistical package for social sciences
CA	Cornu ammonis
OL	Pleomorphic layer
PL	Pyramidal layer
ML	Molecular layer
DML	Dentate molecular layer
GL	Granular layer
DOL	Dentate pleomorphic layer
BDNF	Brain-derived neurotrophic factor

Acknowledgements

The authors are thankful to the members of the Laboratory Animal House Unit of Kasr Al-Aini, Faculty of Medicine, Cairo University.

Author contributions

EAF, STM, SMA were responsible for conducting, monitoring of the experiment and preparation and photographing of histological sections. All authors were responsible for interpretation and analysis of photos and data, writing and revision of the manuscript. All authors read and approved the final manuscript.

Funding
Not applicable.

Availability of data and materials
Available upon a reasonable request.

Declarations

Ethics approval and consent to participate
Animals were housed in Kasr Al-Ainy Animal House & treated according to the guidelines of Cairo University Institutional Animal Care and Use Committee (CU-IACUC). The study approval number: CU-III-F-21-20.

Consent for publication
Not applicable.

Competing interests
The authors declare that they have no competing interests.

Received: 9 March 2023 Accepted: 28 May 2023
Published online: 06 June 2023

References

1. Biondi B, Cooper DS (2019) Thyroid hormone therapy for hypothyroidism. Endocrine 66(1):18–26
2. Chiovato L, Magri F, Carlé A (2019) Hypothyroidism in context: where we've been and where we're going. Adv Ther 36(Suppl 2):47–58
3. Mohan V, Sinha RA, Pathak A, Rastogi L, Kumar P, Pal A, Godbole MM (2012) Maternal thyroid hormone deficiency affects the fetal neocorticogenesis by reducing the proliferating pool, rate of neurogenesis and indirect neurogenesis. Exp Neurol 237(2):477–488
4. Alzoubi KH, Gerges NZ, Aleisa AM, Alkadhi KA (2009) Levothyroxin restores hypothyroidism-induced impairment of hippocampus-dependent learning and memory: behavioral, electrophysiological, and molecular studies. Hippocampus 19(1):66–78
5. Bajaj S, Sachan S, Misra V, Varma A, Saxena P (2014) Cognitive function in subclinical hypothyroidism in elderly. Indian J Endocrinol Metab 18(6):811–814
6. Elbadawy AM, Mansour AE, Abdelrassoul IA, Abdelmoneim RO (2020) Relationship between thyroid dysfunction and dementia. Egypt J Intern Med 32:1–9
7. Toda T, Parylak SL, Linker SB, Gage FH (2019) The role of adult hippocampal neurogenesis in brain health and disease. Mol Psychiatry 24(1):67–87
8. Cooke GE, Mullally S, Correia N, O'Mara SM, Gibney J (2014) Hippocampal volume is decreased in adults with hypothyroidism. Thyroid 24(3):433–440
9. Martínez-Salazar C, Villanueva I, Pacheco-Rosado J, Alva-Sánchez C (2020) Moderate exercise prevents the cell atrophy caused by hypothyroidism in rats. Acta Neurobiol Exp (Wars) 80(1):47–56
10. Zhao M, Liu L, Wang F, Yuan Z, Zhang X, Xu C, Song Y, Guan Q, Gao L, Shan Z, Zhang H, Zhao J (2016) A worthy finding: decrease in total cholesterol and low-density lipoprotein cholesterol in treated mild subclinical hypothyroidism. Thyroid 26(8):1019–1029
11. Chaalal A, Poirier R, Blum D, Laroche S, Enderlin V (2019) Thyroid hormone supplementation restores spatial memory, hippocampal markers of neuroinflammation, plasticity-related signaling molecules, and β-amyloid peptide load in hypothyroid rats. Mol Neurobiol 56(1):722–735
12. Mishra J, Vishwakarma J, Malik R, Gupta K, Pandey R, Maurya SK, Garg A, Shukla M, Chattopadhyay N, Bandyopadhyay S (2021) Hypothyroidism induces interleukin-1-dependent autophagy mechanism as a key mediator of hippocampal neuronal apoptosis and cognitive decline in postnatal rats. Mol Neurobiol 58(3):1196–1211
13. Hossain AO (2019) Carbimazole and its effects on thyroid gland of female rabbits. Indian J Forensic Med Toxicol 13(3):305–311
14. Ochani S, Siddiqui A, Adnan A (2022) Adverse effects of long-term levothyroxine therapy in subclinical hypothyroidism. Ann Med Surg (Lond) 76:103503
15. Fekry E, Awny M, Refaat G, Arafat H (2023) Ameliorative role of Saussurea Lappa root extract "Costus" on thyroid tissue under the toxic effect of carbimazole induced hypothyroidism. Zagazig J Forensic Med 21(1):172–189. https://doi.org/10.21608/zjfm.2023.188310.1139
16. Alva-Sánchez C, Sánchez-Huerta K, Arroyo-Helguera O, Anguiano B, Aceves C, Pacheco-Rosado J (2009) The maintenance of hippocampal pyramidal neuron populations is dependent on the modulation of specific cell cycle regulators by thyroid hormones. Brain Res 1271:27–35
17. Bowerbank SL, Carlin MG, Dean JR (2019) A direct comparison of liquid chromatography-mass spectrometry with clinical routine testing immunoassay methods for the detection and quantification of thyroid hormones in blood serum. Anal Bioanal Chem 411(13):2839–2853
18. Gage GJ, Kipke DR, Shain W (2012) Whole animal perfusion fixation for rodents. J Vis Exp 65:3564
19. Venkataraman P, Selvakumar K, Krishnamoorthy G, Muthusami S, Rameshkumar R, Prakash S, Arunakaran J (2010) Effect of melatonin on PCB (Aroclor 1254) induced neuronal damage and changes in Cu/Zn superoxide dismutase and glutathione peroxidase-4 mRNA expression in cerebral cortex, cerebellum, and hippocampus of adult rats. Neurosci Res 66(2):189–197
20. Suvarna K, Layton C, Bancroft J (2019) The hematoxylins and eosin, Immunohistochemical and immunofluorescent techniques. In: Bancroft's Theory and Practice of Histological Techniques, 8th edn. Elsevier, pp 126–138, 306–336, 337–394.
21. Bologna-Molina R, Mosqueda-Taylor A, Molina-Frechero N, Mori-Estevez AD, Sánchez-Acuña G (2013) Comparison of the value of PCNA and Ki-67 as markers of cell proliferation in ameloblastic tumors. Med Oral Patol Oral Cir Bucal 18(2):e174–e179
22. Diaz-Arrastia R, Wang KK, Papa L, Sorani MD, Yue JK, Puccio AM, McMahon PJ, Inoue T, Yuh EL, Lingsma HF, Maas AI, Valadka AB, Okonkwo DO, Manley GT, Investigators TRACK-TBI (2014) Acute biomarkers of traumatic brain injury: relationship between plasma levels of ubiquitin C-terminal hydrolase-L1 and glial fibrillary acidic protein. J Neurotrauma 31(1):19–25
23. Kwon SE, Chapman ER (2011) Synaptophysin regulates the kinetics of synaptic vesicle endocytosis in central neurons. Neuron 70(5):847–854
24. Mateo RCI, Hennessey JV (2019) Thyroxine and treatment of hypothyroidism: seven decades of experience. Endocrine 66(1):10–17
25. Ge JF, Xu YY, Qin G, Cheng JQ, Chen FH (2016) Resveratrol ameliorates the anxiety- and depression-like behavior of subclinical hypothyroidism rat: possible involvement of the HPT Axis, HPA Axis, and Wnt/β-catenin pathway. Front Endocrinol (Lausanne) 7:44
26. Benvenga S, Di Bari F, Granese R, Antonelli A (2017) Serum thyrotropin and phase of the menstrual cycle. Front Endocrinol (Lausanne) 8:250
27. Sánchez-Huerta K, García-Martínez Y, Vergara P, Segovia J, Pacheco-Rosado J (2016) Thyroid hormones are essential to preserve non-proliferative cells of adult neurogenesis of the dentate gyrus. Mol Cell Neurosci 76:1–10
28. Hammad AY, Adam SIY, Abdelgadir WS (2021) Comparative effects of bisphenol A, Carbimazole and thyroxine administration on the thyroid gland, serum selenium and iodine concentration of Wistar rats. Asian J Res Rep Endocrinol 4(1):8–18
29. Papich MG (2016) Saunders Handbook of Veterinary Drugs. 4th edn. WB Saunders, pp 107–108.
30. Mandyam CD (2023) Hippocampal circuits. In: Neurocircuitry of Addiction, Academic Press, pp 247–288.
31. Nam SM, Kim JW, Yoo DY, Jung HY, Chung JY, Kim DW, Hwang IK, Yoon YS (2018) Hypothyroidism increases cyclooxygenase-2 levels and pro-inflammatory response and decreases cell proliferation and neuroblast differentiation in the hippocampus. Mol Med Rep 17(4):5782–5788
32. El-Ghareeb AA, El-Bakry AM, Ahmed RG, Gaber A (2016) Effects of Zinc Supplementation in Neonatal Hypothyroidism and Cerebellar Distortion Induced by Maternal Carbimazole. *Asian Journal of Applied Sciences*, 4(4). Available at: https://www.ajouronline.com/index.php/AJAS/article/view/4096 (Accessed: 26 April 2023).
33. Torres-Manzo AP, Franco-Colín M, Blas-Valdivia V, Pineda-Reynoso M, Cano-Europa E (2018) Hypothyroidism causes endoplasmic reticulum stress in adult rat hippocampus: a mechanism associated with hippocampal damage. Oxid Med Cell Longev 2018:2089404

34. Khordad E, Alipour F, Beheshti F, Hosseini M, Rajabzadeh AA, Asiaei F, Seghatoleslam M (2018) Vitamin C prevents hypothyroidism associated neuronal damage in the hippocampus of neonatal and juvenile rats: a stereological study. J Chem Neuroanat 93:48–56
35. Blas-Valdivia V, Franco-Colín M, Rojas-Franco P, Chao-Vazquez A, Cano-Europa E (2021) Gallic acid prevents the oxidative and endoplasmic reticulum stresses in the hippocampus of adult-onset hypothyroid rats. Front Pharmacol 12:671614
36. Cattani D, Goulart PB, Cavalli VL, Winkelmann-Duarte E, Dos Santos AQ, Pierozan P, de Souza DF, Woehl VM, Fernandes MC, Silva FR, Gonçalves CA, Pessoa-Pureur R, Zamoner A (2013) Congenital hypothyroidism alters the oxidative status, enzyme activities and morphological parameters in the hippocampus of developing rats. Mol Cell Endocrinol 375(1–2):14–26
37. Abd Allah ES, Gomaa AM, Sayed MM (2014) The effect of omega-3 on cognition in hypothyroid adult male rats. Acta physiol Hung 101(3):362–376
38. Yildirim AB, Ozdamar S, Yalcin B, Karabulut D (2019) Changes in MAP-2 and GFAP immunoreactivity in pup hippocampus during prepubertal and pubertal periods caused by maternal subclinical hypothyroidism. Eur J Anat 23(1):27–40
39. Kapoor R, Fanibunda SE, Desouza LA, Guha SK, Vaidya VA (2015) Perspectives on thyroid hormone action in adult neurogenesis. J Neurochem 133(5):599–616
40. Remaud S, Gothié JD, Morvan-Dubois G, Demeneix BA (2014) Thyroid hormone signaling and adult neurogenesis in mammals. Front Endocrinol (Lausanne) 5:62
41. Beckervordersandforth R, Zhang CL, Lie DC (2015) Transcription-factor-dependent control of adult hippocampal neurogenesis. Cold Spring Harb Perspect Biol 7(10):a018879
42. Tanaka T, Masubuchi Y, Okada R, Nakajima K, Nakamura K, Masuda S, Nakahara J, Maronpot RR, Yoshida T, Koyanagi M, Hayashi SM, Shibutani M (2019) Ameliorating effect of postweaning exposure to antioxidant on disruption of hippocampal neurogenesis induced by developmental hypothyroidism in rats. J Toxicol Sci 44(5):357–372
43. Korhonen P, Kanninen KM, Lehtonen Š, Lemarchant S, Puttonen KA, Oksanen M, Dhungana H, Loppi S, Pollari E, Wojciechowski S, Kidin I, García-Berrocoso T, Giralt D, Montaner J, Koistinaho J, Malm T (2015) Immunomodulation by interleukin-33 is protective in stroke through modulation of inflammation. Brain Behav Immun 49:322–336
44. Iglesias J, Morales L, Barreto GE (2017) Metabolic and inflammatory adaptation of reactive astrocytes: role of PPARs. Mol Neurobiol 54(4):2518–2538
45. Noda M (2015) Possible role of glial cells in the relationship between thyroid dysfunction and mental disorders. Front Cell Neurosci 9:194
46. Mancini A, Di Segni C, Raimondo S, Olivieri G, Silvestrini A, Meucci E, Currò D (2016) Thyroid hormones, oxidative stress, and inflammation. Mediat Inflamm 2016:6757154
47. Morte B, Gil-Ibáñez P, Bernal J (2018) Regulation of gene expression by thyroid hormone in primary astrocytes: factors influencing the genomic response. Endocrinology 159(5):2083–2092
48. Gudi V, Gai L, Herder V, Tejedor LS, Kipp M, Amor S, Sühs KW, Hansmann F, Beineke A, Baumgärtner W, Stangel M, Skripuletz T (2017) Synaptophysin is a reliable marker for axonal damage. J Neuropathol Exp Neurol 76(2):109–125
49. Gong J, Dong J, Wang Y, Xu H, Wei W, Zhong J, Liu W, Xi Q, Chen J (2010) Developmental iodine deficiency and hypothyroidism impair neural development, up-regulate caveolin-1 and down-regulate synaptophysin in rat hippocampus. J Neuroendocrinol 22(2):129–139
50. Chaalal A, Poirier R, Blum D, Gillet B, Le Blanc P, Basquin M, Buée L, Laroche S, Enderlin V (2014) PTU-induced hypothyroidism in rats leads to several early neuropathological signs of Alzheimer's disease in the hippocampus and spatial memory impairments. Hippocampus 24(11):1381–1393
51. Baldwin KT, Eroglu C (2017) Molecular mechanisms of astrocyte-induced synaptogenesis. Curr Opin Neurobiol 45:113–120
52. Verkhratsky A, Rodríguez-Arellano JJ, Parpura V, Zorec R (2017) Astroglial calcium signalling in Alzheimer's disease. Biochem Biophys Res Commun 483(4):1005–1012
53. Raymaekers SR, Darras VM (2017) Thyroid hormones and learning-associated neuroplasticity. Gen Comp Endocrinol 247:26–33
54. Wang F, Zeng X, Zhu Y, Ning D, Liu J, Liu C, Jia X, Zhu D (2015) Effects of thyroxine and donepezil on hippocampal acetylcholine content, acetylcholinesterase activity, synaptotagmin-1 and SNAP-25 expression in hypothyroid adult rats. Mol Med Rep 11:775–782
55. Tang H, Zhang Y, Yu X, Song J, Xu C, Wan Y (2011) Changes in growth hormone (GH), GH receptor, and GH signal transduction in hippocampus of congenital hypothyroid rats. J Neurosci Res 89(2):248–255
56. Mohamed DA, Ahmed SM (2018) Donepezil improves histological and biochemical changes in the hippocampus of adult hypothyroid male rats. Egypt J Histol 41(4):445–458
57. Guo Y, Wan SY, Zhong X, Zhong MK, Pan TR (2014) Levothyroxine replacement therapy with vitamin E supplementation prevents the oxidative stress and apoptosis in hippocampus of hypothyroid rats. Neuro Endocrinol Lett 35(8):684–690
58. Wrann CD, White JP, Salogiannnis J, Laznik-Bogoslavski D, Wu J, Ma D, Lin JD, Greenberg ME, Spiegelman BM (2013) Exercise induces hippocampal BDNF through a PGC-1a/FNDC5 pathway. Cell Metab 18(5):649–659
59. Marosi K, Mattson MP (2014) BDNF mediates adaptive brain and body responses to energetic challenges. Trends Endocrinol Metab 25(2):89–98
60. Stepien BK, Huttner WB (2019) Transport, metabolism, and function of thyroid hormones in the developing mammalian brain. Front Endocrinol (Lausanne) 10:209
61. Mayerl S, Heuer H (2020) Hippocampal neurogenesis requires cell-autonomous thyroid hormone signaling. Stem Cell Rep 14(5):845–860
62. Montero-Pedrazuela A, Venero C, Lavado-Autric R, Fernández-Lamo I, García-Verdugo JM, Bernal J, Guadaño-Ferraz A (2006) Modulation of adult hippocampal neurogenesis by thyroid hormones: implications in depressive-like behavior. Mol Psychiatry 11(4):361–371
63. Kim SJ, Son TG, Park HR, Park M, Kim MS, Kim HS, Chung HY, Mattson MP, Lee J (2008) Curcumin stimulates proliferation of embryonic neural progenitor cells and neurogenesis in the adult hippocampus. J Biol Chem 283(21):14497–14505
64. Seyedhosseini Tamijani SM, Beirami E, Ahmadiani A, Dargahi L (2019) Thyroid hormone treatment alleviates the impairments of neurogenesis, mitochondrial biogenesis and memory performance induced by methamphetamine. Neurotoxicology 74:7–18
65. Fan WJ, Yan MC, Wang L, Sun YZ, Deng JB, Deng JX (2018) Synaptic aging disrupts synaptic morphology and function in cerebellar Purkinje cells. Neural Regen Res 13(6):1019–1025

Publisher's Note